PROCEEDINGS OF SCIENCE

Determining the QCD coupling from lattice vacuum polarization

Renwick J. Hudspith,[a] **Randy Lewis**[*,a] **Kim Maltman**[b,c] **and Eigo Shintani**[d]

[a] *Department of Physics and Astronomy, York University, Toronto, ON, M3J 1P3, Canada*
[b] *Department of Mathematics and Statistics, York University, Toronto, ON, M3J 1P3, Canada*
[c] *CSSM, University of Adelaide, Adelaide, SA, 5005, Australia*
[d] *RIKEN Advanced Institute for Computational Science, Kobe, Hyogo 650-0047, Japan*
E-mail: renwick.james.hudspith@googlemail.com, randy.lewis@yorku.ca, kmaltman@yorku.ca, shintani@riken.jp

The QCD coupling appears in the perturbative expansion of the current-current two-point (vacuum polarization) function. Any lattice calculation of vacuum polarization is plagued by several competing non-perturbative effects at small momenta and by discretization errors at large momenta. We work in an intermediate region, computing the vacuum polarization for many off-axis momentum directions on the lattice. Having many momentum directions provides a way to monitor and account for lattice artifacts. Our results are competitive with, and have certain systematic advantages over, the alternate phenomenological determination of the strong coupling from the same light quark vacuum polarization produced by sum rule analyses of hadronic τ decay data.

The 33rd International Symposium on Lattice Field Theory
14 -18 July 2015
Kobe International Conference Center, Kobe, Japan

[*]Speaker.

© Copyright owned by the author(s) under the terms of the Creative Commons Attribution-NonCommercial-ShareAlike Licence.

arXiv:1510.04890v1 [hep-lat] 16 Oct 2015

1. Motivation

α_s is a fundamental parameter of QCD and its numerical value is crucial input for most practical calculations in particle physics. Interpretation of experimental data requires the value of α_s to handle QCD backgrounds. Several lattice QCD methods have been employed to determine α_s, including the short-distance QCD potential, Wilson loops, the Schrödinger functional, the ghost-gluon vertex, current two-point functions with heavy valence quarks, and vacuum polarization at short distances. For a review and references, see [1].

Our focus for the present work is the method of vacuum polarization at short distances, studied as a function of Euclidean Q^2, as pioneered by Shintani and collaborators in a sequence of papers [2, 3, 4]. Related studies can be found in [5, 6]. The perturbative expression is a function of α_s. At small Q^2, there are important non-perturbative (NP) contributions in addition to perturbation theory. At large Q^2, there are important lattice artifacts in addition to perturbation theory.

Previous research [2, 3, 4] used Q^2 as low as about 1 GeV^2 and included NP contributions in the fit via the operator product expansion (OPE). This is problematic if successive OPE terms have comparable sizes with alternating signs and, perhaps surprisingly, this phenomenon really can occur, as illustrated by sum rule fit results for the light quark V+A polarization: [7]

$$\Pi^{(1+0)}_{\text{OPE}}(Q^2) = \sum_{k=0}^{\infty} \frac{C_{2k}}{Q^{2k}}, \tag{1.1}$$

$$C_{4,V+A} = +0.00268\ \text{GeV}^4, \tag{1.2}$$

$$C_{6,V+A} = -0.0125\ \text{GeV}^6, \tag{1.3}$$

$$C_{8,V+A} = +0.0349\ \text{GeV}^8, \tag{1.4}$$

$$C_{10,V+A} = -0.0832\ \text{GeV}^{10}, \tag{1.5}$$

$$C_{12,V+A} = +0.161\ \text{GeV}^{12}, \tag{1.6}$$

$$C_{14,V+A} = -0.191\ \text{GeV}^{14}, \tag{1.7}$$

$$C_{16,V+A} = -0.233\ \text{GeV}^{16}. \tag{1.8}$$

For numerical values of $C_{6,V}$ and $C_{8,V}$, see Table III of [7]. This sequence of coefficients only produces a manageable OPE series for sufficiently large Q^2. With this potential danger in mind, we restrict our attention to Q^2 values large enough that all NP OPE terms are negligible in the present analysis.

2. Method

The vector current two-point correlation function with I=1 and m_u=m_d is

$$\langle V_\mu V_\nu \rangle \equiv \Pi_{\mu\nu}(Q) = (Q^2\delta_{\mu\nu} - Q_\mu Q_\nu)\Pi(Q^2). \tag{2.1}$$

The QCD coupling will be obtained from $\Pi(Q^2)$. There is a close relation to the τ decay determination of α_s, which uses experimental spectral data and finite-energy sum rule (FESR) analysis of the same $\Pi(Q^2)$, but here we have certain systematic advantages. In particular, our lattice calculation is performed directly at Euclidean Q^2 whereas the FESR approach [8] requires calculation on

Table 1: The lattices used in this study are characterized by spatial extent L, temporal extent T, gauge coupling β, bare quark masses m_s and m_ℓ, lattice spacing a, vector renormalization constant Z_V, and number of configurations $n_{\rm conf}$.

$L^3\times T$	β	m_s	m_ℓ	a^{-1} [GeV]	Z_V	$n_{\rm conf}$
$24^3\times 64$	2.13	0.04	0.005,0.01,0.02	1.78	0.714	900
$32^3\times 64$	2.25	0.03	0.004,0.006,0.008	2.38	0.745	940

a circle in the complex Q^2 plane that comes infinitesimally close to the Minkowski axis. The OPE is not a good description of Minkowski physics, so the FESR approach relies on certain weights that are chosen to minimize the impact of physics near the Minkowski axis. The present lattice approach avoids the issue entirely by working exclusively with Euclidean Q^2.

The perturbative expression up to 6 loops, in the $\overline{\rm MS}$ renormalization scheme at scale μ, is

$$\Pi(Q^2) = C - \frac{1}{4\pi^2}\left(t + \sum_{k=1}^{5}\left(\frac{\alpha_s(\mu)}{\pi}\right)^k \sum_{m=0}^{k-1} c^A_{km}\frac{t^{m+1}}{m+1}\right) \tag{2.2}$$

where C is a constant and $t = \ln(Q^2/\mu^2)$. All coefficients are known except c^A_{50}, which has been estimated [9].

Discretization errors grow as Q^2 increases, but they can be managed. Choosing the momentum to be along a single lattice axis is particularly undesirable, so we have generated $\Pi(Q^2)$ for all possible momenta Q_μ. With those data in hand, we define $\hat{v} = (1,1,1,1)/2$ and calculate

$$(Q_\perp)_\mu = Q_\mu - (Q\cdot\hat{v})\hat{v}_\mu\,. \tag{2.3}$$

If Q_μ points along a lattice diagonal then $Q_\perp = 0$. For fixed $|Q^2|$, those Q_μ options aligned most closely with $\hat{v}_\mu$ have the smallest lattice artifacts so we implement a maximum radius $|Q_\perp|_{\rm max}$.

We handle O(4)-breaking lattice artifacts via reflection averaging:

$$\Pi_{\rm lat}(Q^2) = \frac{1}{12}\sum_{\mu=x,y,z,t}\sum_{\nu\neq\mu}\left(\frac{\Pi_{\mu\nu}(Q) - \Pi_{\mu\nu}(R_\mu Q)}{2Q_\mu Q_\nu}\right) \tag{2.4}$$

where R_μ is a reflection operator in the μ direction. In practice, division by zero is no problem because any Q having a vanishing component will be beyond the maximum radius $|Q_\perp|_{\rm max}$. After reflection averaging, there are still O(4)-preserving artifacts that remain to be fitted:

$$\Pi_{\rm lat}(Q^2) = \Pi(Q^2) + c_1 a^2 Q^2 + c_2 a^4 Q^4 + \ldots \tag{2.5}$$

We use ensembles from the RBC and UKQCD Collaborations [10] with parameters shown in Table 1. We calculate $\langle V^L_\mu V^C_\nu\rangle$. The local current V^L removes a contact term and the conserved current V^C preserves the Ward-Takahashi identity:

$$\sum_\nu \hat{Q}_\nu e^{iQ_\nu/2}\Pi_{\mu\nu} = 0 \;\text{ where }\; \hat{Q}_\nu = 2\sin(Q_\nu/2)\,. \tag{2.6}$$

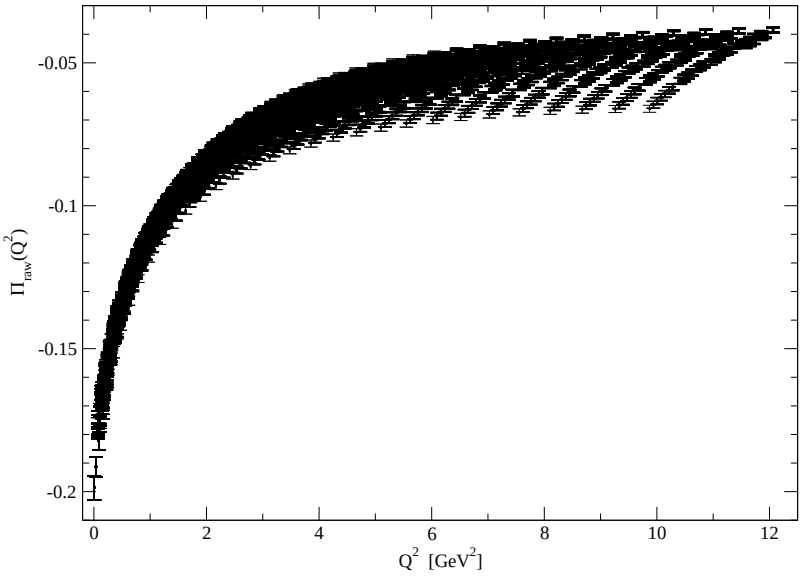

Figure 1: Raw data for vacuum polarization obtained from 5 configurations for $\bar{s}s$ valence quarks. Momenta along a single lattice axis are near the bottom of the fishbone pattern. Momenta along the diagonal of the lattice are near the top of the fishbone pattern.

Because $\Pi(Q^2)$ only depends on α_s at subleading orders, we prefer to use instead a renormalization-independent function where α_s appears at leading order:

$$\Delta(Q^2, Q^2_{\text{ref}}) \equiv -4\pi^2 \left(\frac{\Pi_{\text{lat}}(Q^2) - \Pi_{\text{lat}}(Q^2_{\text{ref}})}{\ln(\hat{Q}^2/\hat{Q}^2_{\text{ref}})} \right) - 1 \tag{2.7}$$

$$= \frac{\alpha_s(\mu)}{\pi} + \text{ higher orders.} \tag{2.8}$$

3. Results and systematics

The raw lattice data obtained from

$$\Pi_{\text{raw}}(Q^2) = \frac{-1}{3\hat{Q}^2} \left(\delta_{\mu\nu} - \frac{4\hat{Q}_\mu \hat{Q}_\nu}{\hat{Q}^2} \right) \Pi_{\mu\nu}(Q^2) \tag{3.1}$$

show a fishbone pattern due to lattice artifacts, as displayed in Fig. 1, making it difficult to extract physical vacuum polarization as a single-valued function of Q^2. In contrast, the reflection averaging of Eq. (2.4) combined with an appropriate choice for $|Q_\perp|_{\max}$ produces the smooth curves displayed in Fig. 2 that retain a large number of usable Q^2 values.

For the $32^3 \times 64$ ensemble, which has the smaller lattice spacing, good fits are obtained with just 2 fit parameters. The fit function is Eq. (2.5) with parameters $\alpha_s(\mu)$ and c_1. All other c_i are set to zero because c_1 is sufficient to represent all of the lattice artifacts in this reflection-averaged data set. Figure 3 shows the resulting value for $\alpha_s(\mu)$ as a single red data point that appears on 6 different panels. Panel (a) indicates that the result is not sensitive to changes in the light quark mass.

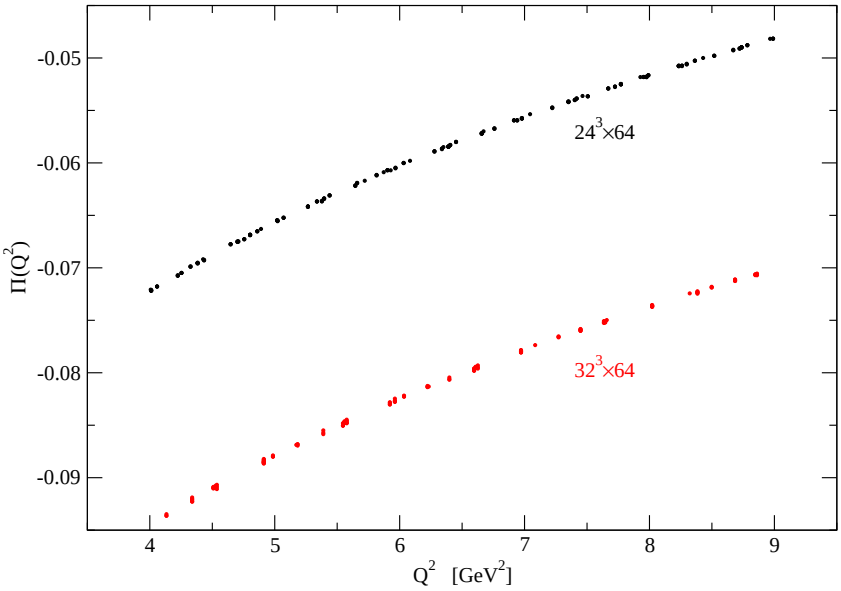

Figure 2: Data for vacuum polarization after use of Eq. (2.4) and an appropriate choice for $|Q_\perp|_{\max}$.

Panel (b) shows insensitivity to our choice of $|Q_\perp|_{\max}$; the error bar grows if $|Q_\perp|_{\max}$ becomes too small because an agressive cut leaves too few data points in the fit.

Experience from τ decay phenomenology says $Q^2_{\min} \gtrsim 4$ GeV^2 is required to avoid the OPE dangers described above, and panel (c) shows that these lattice results are consistent with that expectation. Results should be insensitive to $Q^2_{\max}$ if lattice artifacts are under control, and panel (d) verifies this for our data.

Equation (2.7) requires a subtraction point Q^2_{ref}, and panel (e) shows the statistical variation obtained from choosing any single direction for Q_{ref} instead of averaging over all equivalent options.

Panel (f) displays the systematic shift in α_s that would come from truncating the perturbative expansion at a lower order. Although the red point does receive input from the estimated coefficient c^A_{50}, our result is insensitive to its precise value.

Results displayed in Fig. 3 are for the $32^3\times64$ ensemble with $a^{-1} = 2.38$ GeV. We should perform a similar analysis for $24^3\times64$ with $a^{-1} = 1.78$ GeV but two issues arise: (1) a two-parameter fit (Eq. (2.5) with α_s and c_1) does not describe the data well, and (2) a three-parameter fit (Eq. (2.5) with α_s, c_1 and c_2) allows a huge error bar for α_s. The situation is displayed graphically in Fig. 4. Unfortunately, we must conclude that a two-parameter fit is not sufficient for the coarse lattice, and that the statistical precision is not presently available to get α_s from the 3-parameter fit.

4. Numerical result for α_s

The analysis reported here gives

$$\frac{\alpha_s(2\,\text{GeV})}{\pi} = 0.0889 \pm 0.0035 \tag{4.1}$$

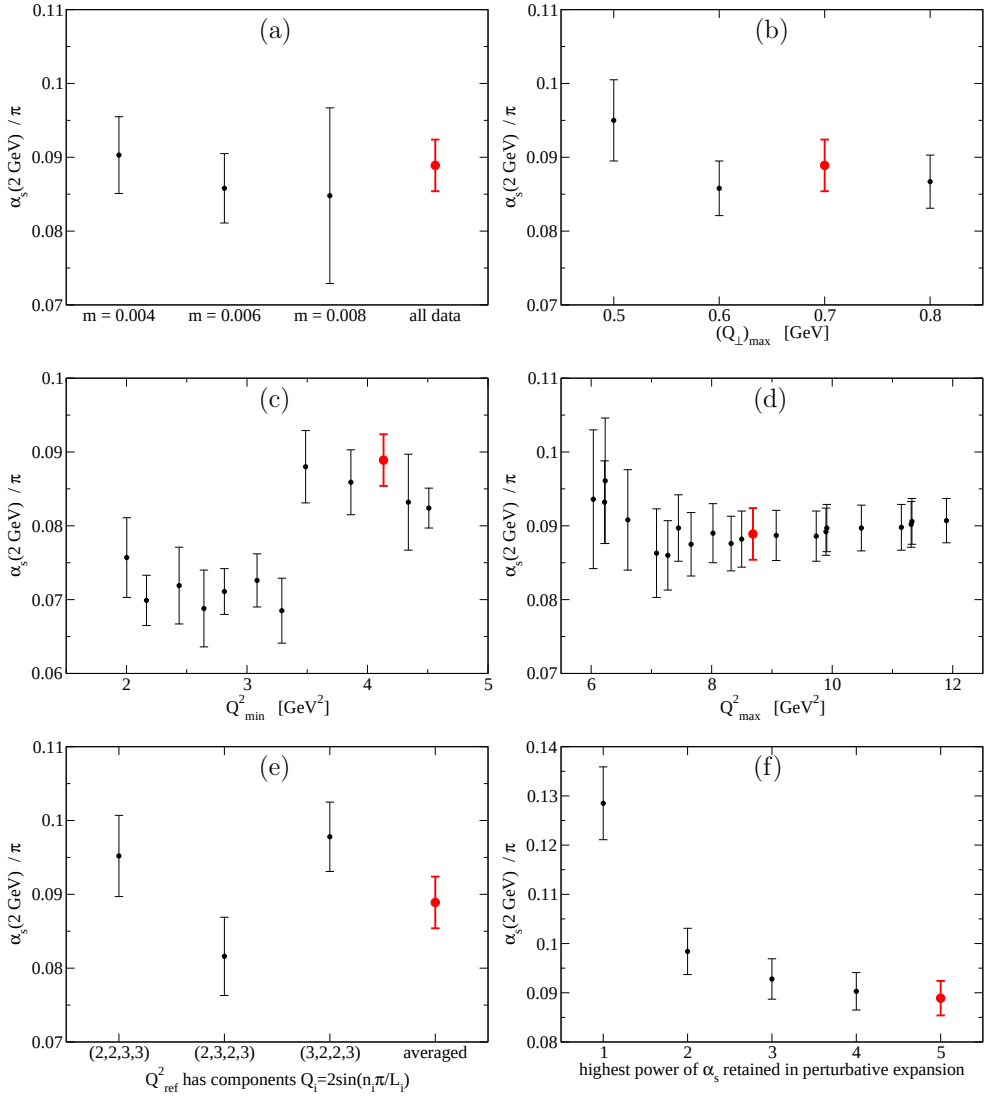

Figure 3: The strong coupling obtained from the $32^3 \times 64$ ensemble (in red), and its dependence on 6 systematics as explained in the text.

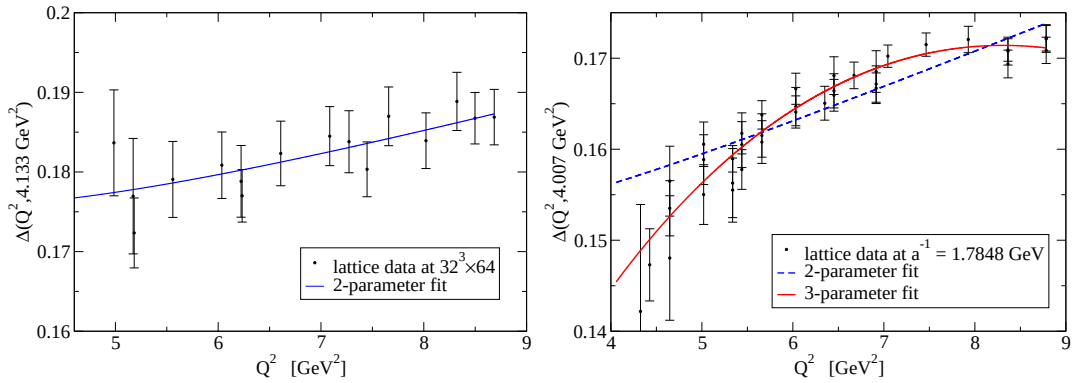

Figure 4: The left panel shows a useful 2-parameter fit to the finer ensemble. The right panel shows that the coarser ensemble requires a third parameter in the fit.

and running to the τ mass gives

$$\alpha_s^{(3)}(m_\tau) = 0.296 \pm 0.013 \tag{4.2}$$

which is in excellent agreement with results that use τ decay data from experiment for an alternate analysis of the same $\Pi(Q^2)$. In particular, the recent continuum FESR analysis of the 2013/14 corrected and updated ALEPH hadronic τ decay data arrived at [8]

$$\alpha_s^{(3)}(m_\tau) = \begin{cases} 0.296 \pm 0.010 & \text{[fixed-order perturbation theory]}, \\ 0.310 \pm 0.014 & \text{[contour-improved perturbation theory]}. \end{cases} \tag{4.3}$$

Running our result in Eq. (4.1) to m_Z in the 5-flavor theory gives $\alpha_s^{(5)}(m_Z) = 0.1155 \pm 0.0018$. For comparison, the FLAG Working Group result is [1] $\alpha_s^{(5)}(m_Z) = 0.1184 \pm 0.0012$.

5. Summary

We have presented a new implementation to obtain α_s from vacuum polarization at short distances. It avoids the danger of systematic errors that could arise in low-scale fits as a result of alternating-sign higher-dimension OPE contributions. Our method needs $\Pi(Q^2)$ for many off-axis lattice directions. Our numerical results are competitive with the determination of α_s from τ decay. In the future, we hope to use data from finer lattices since this will allow a study of the continuum limit.

Acknowledgments: This work was supported in part by NSERC of Canada.

References

[1] S. Aoki *et al.*, Eur. Phys. J. C **74**, 2890 (2014) [arXiv:1310.8555 [hep-lat]].

[2] E. Shintani *et al.* [JLQCD and TWQCD Collaborations], Phys. Rev. D **79**, 074510 (2009) [arXiv:0807.0556 [hep-lat]].

[3] E. Shintani, S. Aoki, H. Fukaya, S. Hashimoto, T. Kaneko, T. Onogi and N. Yamada, Phys. Rev. D **82**, 074505 (2010) [Phys. Rev. D **89**, 099903 (2014)] [arXiv:1002.0371 [hep-lat]].

[4] E. Shintani, H. J. Kim, T. Blum and T. Izubuchi, PoS LATTICE **2013**, 487 (2014).

[5] G. Herdoiza, H. Horch, B. Jäger and H. Wittig, PoS LATTICE **2013**, 444 (2014).

[6] A. Francis, G. Herdoíza, H. Horch, B. Jäger, H. B. Meyer and H. Wittig, PoS LATTICE **2014**, 163 (2014) [arXiv:1412.6934 [hep-lat]].

[7] D. Boito, M. Golterman, K. Maltman, J. Osborne and S. Peris, Phys. Rev. D **91**, no. 3, 034003 (2015) [arXiv:1410.3528 [hep-ph]].

[8] D. Boito, M. Golterman, K. Maltman, J. Osborne and S. Peris, Nucl. Part. Phys. Proc. **260**, 134 (2015) [arXiv:1410.8415 [hep-ph]].

[9] P. A. Baikov, K. G. Chetyrkin and J. H. Kuhn, Phys. Rev. Lett. **101**, 012002 (2008) [arXiv:0801.1821 [hep-ph]].

[10] R. Arthur *et al.* [RBC and UKQCD Collaborations], Phys. Rev. D **87**, 094514 (2013) [arXiv:1208.4412 [hep-lat]].